

PAPER • OPEN ACCESS

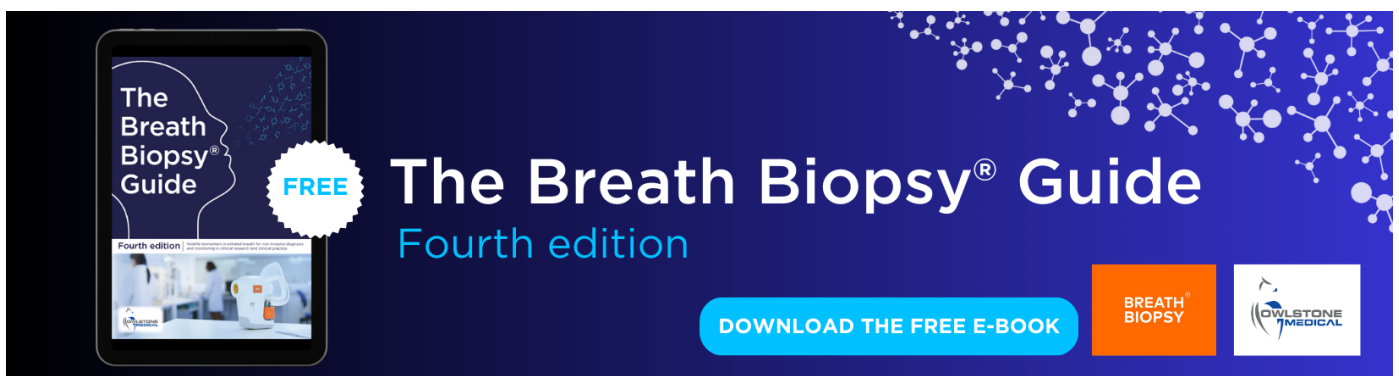
Modeling cloud-to-ground lightning probability in Alaskan tundra through the integration of Weather Research and Forecast (WRF) model and machine learning method

To cite this article: Jiaying He and Tatiana V Loboda 2020 *Environ. Res. Lett.* **15** 115009

View the [article online](#) for updates and enhancements.

You may also like

- [Exposure to cold temperature affects the spring phenology of Alaskan deciduous vegetation types](#)
Mingjie Shi, Nicholas C Parazoo, Su-Jong Jeong et al.
- [Circumpolar spatio-temporal patterns and contributing climatic factors of wildfire activity in the Arctic tundra from 2001–2015](#)
Arif Masrur, Andrey N Petrov and John DeGroote
- [Siberian taiga and tundra fire regimes from 2001–2020](#)
Anna C Talucci, Michael M Loranty and Heather D Alexander



The Breath Biopsy® Guide
Fourth edition

FREE

DOWNLOAD THE FREE E-BOOK

BREATH BIOPSY

OWLSTONE MEDICAL

Environmental Research Letters



PAPER

OPEN ACCESS

RECEIVED
10 April 2020

REVISED
12 August 2020

ACCEPTED FOR PUBLICATION
28 September 2020

PUBLISHED
2 November 2020

Original content from this work may be used under the terms of the [Creative Commons Attribution 4.0 licence](#).

Any further distribution of this work must maintain attribution to the author(s) and the title of the work, journal citation and DOI.



Modeling cloud-to-ground lightning probability in Alaskan tundra through the integration of Weather Research and Forecast (WRF) model and machine learning method

Jiaying He and Tatiana V Loboda

Department of Geographical Sciences, University of Maryland, 2181 Samuel J. Lefrak Hall, 7251 Preinkert Drive, College Park, MD, United States of America

E-mail: hjy0608@terpmail.umd.edu

Keywords: Alaskan tundra, cloud-to-ground lightning, empirical-dynamic modeling, lightning-ignited wildfire, Weather Research and Forecast (WRF), random forest

Supplementary material for this article is available [online](#)

Abstract

Wildland fires exert substantial impacts on tundra ecosystems of the high northern latitudes (HNL), ranging from biogeochemical impact on climate system to habitat suitability for various species. Cloud-to-ground (CG) lightning is the primary ignition source of wildfires. It is critical to understand mechanisms and factors driving lightning strikes in this cold, treeless environment to support operational modeling and forecasting of fire activity. Existing studies on lightning strikes primarily focus on Alaskan and Canadian boreal forests where land-atmospheric interactions are different and, thus, not likely to represent tundra conditions. In this study, we designed an empirical-dynamical method integrating Weather Research and Forecast (WRF) simulation and machine learning algorithm to model the probability of lightning strikes across Alaskan tundra between 2001 and 2017. We recommended using Thompson 2-moment and Mellor–Yamada–Janjic schemes as microphysics and planetary boundary layer parameterizations for WRF simulations in the tundra. Our modeling and forecasting test results have shown a strong capability to predict CG lightning probability in Alaskan tundra, with the values of area under the receiver operator characteristics curves above 0.9. We found that parcel lifted index and vertical profiles of atmospheric variables, including geopotential height, dew point temperature, relative humidity, and velocity speed, important in predicting lightning occurrence, suggesting the key role of convection in lightning formation in the tundra. Our method can be applied to data-scarce regions and support future studies of fire potential in the HNL.

1. Introduction

Wildland fire is a dominant disturbance across boreal forest and tundra ecosystems in the high northern latitudes (HNL; Goetz *et al* 2005, Bond-Lamberty *et al* 2007, French *et al* 2015). Tundra fires can alter ecosystem functioning and drive environmental changes in carbon cycling and energy budget (Mack *et al* 2011, Bret-Harte *et al* 2013, Pearson *et al* 2013, Jones *et al* 2015, French *et al* 2016). Specifically, they can release large stores of carbon locked in organic soil and permafrost. For example, the 2007 Anaktuvuk River fire in Alaska burned 1039 km² and released ~2.1 Tg carbon into the atmosphere (Mack *et al* 2011). Although much rarer and generally less severe than boreal fires,

they are common, particularly in Alaska. Between 2001 and 2015, Alaskan tundra has burnt about 54% of 10 260 km² burned area in the tundra worldwide (He *et al* 2019). Additionally, post-fire recovery for critical components of the tundra ecosystem can last for several decades, which is comparable to that of the boreal forests (Racine *et al* 1987, Jandt *et al* 2008). Thus, tundra fires can impact long-term winter forage availability, particularly lichen, for caribou, which will subsequently influence the subsistence resources of local human communities (Gustine *et al* 2014, Bliss and Hu 2020).

Fires in the remote and generally inaccessible HNL are primarily ignited by cloud-to-ground (CG) lightning flashes (French *et al* 2015, Veraverbeke *et al*

2017), also known as lightning strikes. Future projections indicate potential increase of lightning under climate warming (Price and Rind 1994a, Romps *et al* 2014), which will subsequently lead to more fire occurrences and larger burned areas in the HNL (Wotton *et al* 2010, Krause *et al* 2014, French *et al* 2015, Veraverbeke *et al* 2017). Numerous studies have explored the driving factors of lightning strikes and developed predictive models (Burrows *et al* 2005, Blouin *et al* 2016) for Alaskan and Canadian boreal forests. However, considerably less is known about factors driving CG lightning for the treeless tundra. The substantial differences in surface conditions between tree-dominated and treeless landscapes (Dissing and Verbyla 2003, Beringer *et al* 2005, Van Heerwaarden and Teuling 2014, Rivas Soriano *et al* 2019) imply that understanding lightning processes in the boreal forests is not necessarily readily transferable to the tundra. Therefore, tundra-focused studies are critical for enhancing the modeling capability of lightning and fire potential, and assisting wildfire management efforts in the future.

Typically, lightning formation is associated with atmospheric convection in cumulonimbus clouds (Anderson 1992). Lightning flashes are generated through buildup, separation, and transfer procedures of electric charges between cloud particles (Saunders 2008, Yair 2008). The occurrence and intensity of lightning are generally related to factors such as convective cloud development, cloud structure, and hydrometeor attributes (Price and Rind 1994b, Baker *et al* 1999, Buiat *et al* 2017). However, explicit simulation and prediction of the electrification processes can be computationally expensive (Zepka *et al* 2014). Further efforts are also required to comprehensively understand the detailed microphysical procedures contributing to the charge accumulation (Rakov and Uman 2003, Saunders 2008). Efforts on modeling lightning activity thus primarily rely on developing relationships with observed or model-resolved parameters related to convective activities and cloud microphysical properties.

Classificatory schemes or regression methods developed with convective indices or weather conditions were among the earliest lightning modeling attempts (Anderson 1991, Sly 1965, Reap and Foster 1979, Fuquay 1980, Reap and Macgorman 1989). With the development of numerical weather prediction (NWP) models, lightning schemes based on microphysics principles have been parameterized within models from regional to global scales (Price and Rind 1994b, Barthe *et al* 2010, Yair *et al* 2010, Lynn *et al* 2012, Wong *et al* 2013). Simple strategies were also designed with Weather Research and Forecast (WRF) simulations (Zepka *et al* 2014, Giannaros *et al* 2015). In addition to physical parameterizations, empirical-based methods such as logistic regression (Shafer and Fuelberg 2006, Bates *et al* 2018) and random forest (RF; Blouin *et al* 2016, Schön *et al*

2018) were adopted to model lightning based on meteorological conditions and thunderstorm characteristics. Opportunities for integrating dynamic NWP and statistical models have been explored to improve the modeling capability of lightning potential. Burrows *et al* (2005) trained tree-structured regression models to forecast lightning probability based on the Global Environmental Multiscale (GEM) model. Sousa *et al* (2013) and Gijben *et al* (2017) also combined WRF with logistic regression to develop a statistical-dynamical method for CG lightning prediction in different regions.

Due to the remoteness of tundra, meteorological observations are very sparsely distributed and thus unsuitable for describing the spatial variation of tundra conditions. Although reanalysis products ensure spatial-temporal consistency, their performances are limited by the coarse resolution, limited availability of observations, and uncertainty of diagnostic variables (Dee *et al* 2016). Therefore, purely empirical models trained with these data are inappropriate for lightning modeling in data-scarce regions like tundra. Although NWP has not been specifically adopted in tundra studies, existing research has demonstrated its suitability and effectiveness for modeling lightning potential (Reap 1991, Burrows *et al* 2005) and fire danger (Mölders 2010, Di Giuseppe *et al* 2016) in boreal forests. In this study, we aim to understand what atmospheric factors affect the CG lightning probability in Alaskan tundra from 2001 to 2017 and to model the probability by integrating WRF and RF.

2. Study area

We defined Alaskan tundra using the Circumpolar Arctic Vegetation Map (CAVM; figure 1(a); Walker *et al* 2005). Fire regimes vary by year and across different tundra regions (figure 2). In Alaska, more than 99% of the lightning strikes occur from May to August (Reap 1991, Mcguiney *et al* 2005). Lightning activity shows a typical diurnal pattern from noon until midnight with a peak between 4 pm and 8 pm. Elevation and forest cover can affect the spatial variation of lightning strikes in Alaska by altering the convective activity (Dissing and Verbyla 2003). In particular, large-scale atmospheric instability and local convergence are the primary contributors to the formation thunderstorm of lightning (Reap 1991).

3. Materials and methods

We designed an empirical-dynamical method using WRF-simulated atmospheric variables to model CG lightning probability and understand its driving factors in Alaskan tundra. We first conducted a sensitivity analysis to identify optimal WRF parameterizations that best describes tundra meteorological conditions. We then ran WRF and

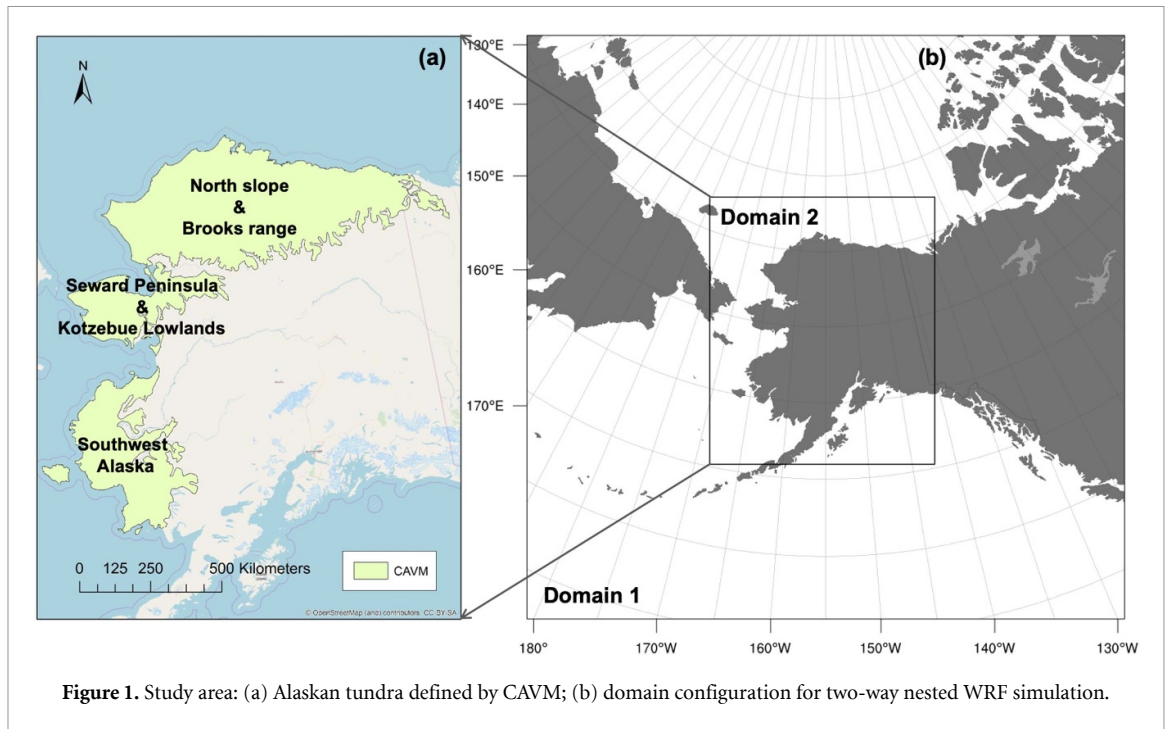


Figure 1. Study area: (a) Alaskan tundra defined by CAVM; (b) domain configuration for two-way nested WRF simulation.

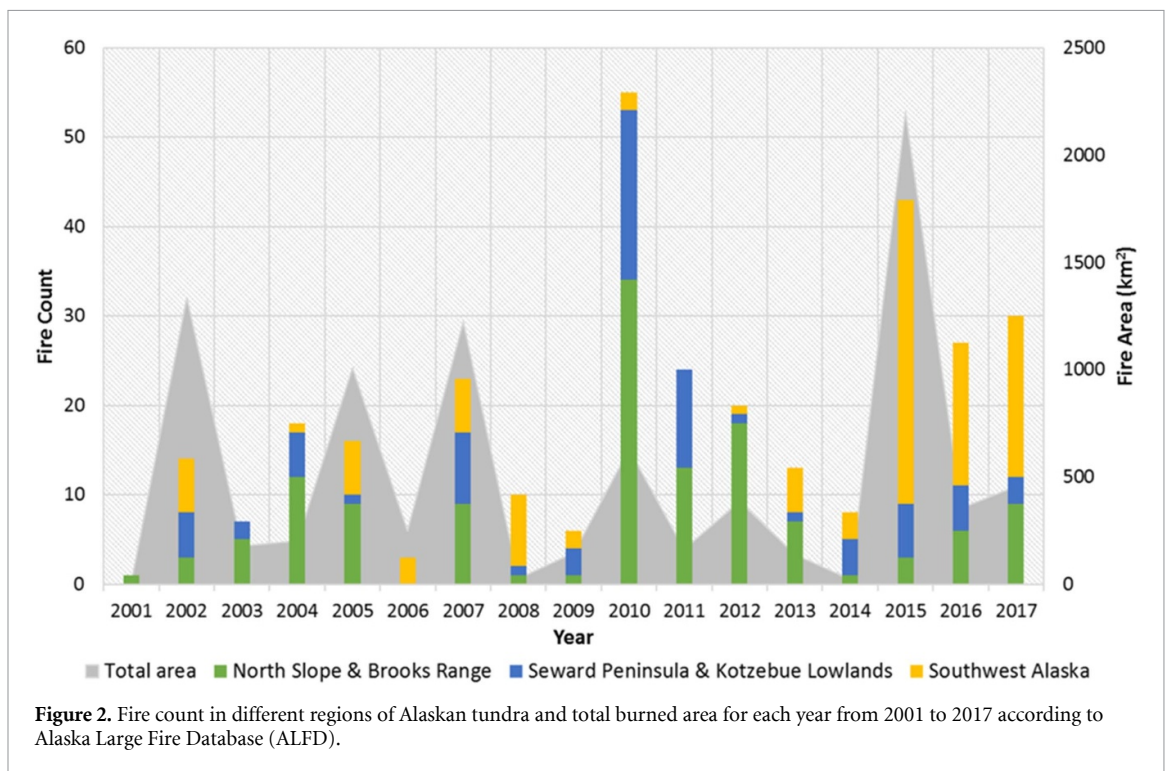


Figure 2. Fire count in different regions of Alaskan tundra and total burned area for each year from 2001 to 2017 according to Alaska Large Fire Database (ALFD).

developed RF models for predicting CG lightning probability.

3.1. CG lighting observations

We obtained lightning data from the Alaska Lightning Detection Network (ALDN; Fronterhouse 2012), with a detection efficiency better than 5 km and positional accuracy higher than 70% (Reap 1991, Dissing and Verbyla 2003). The system has been updated to improve detection performance (Fronterhouse 2012). Devices employed before 2012, developed by

Vaisala, Inc., recorded lightning flash with multiplicity (i.e., lightning strikes per flash). The new system, provided by TOA Systems, Inc., records lightning strikes instead (Fronterhouse 2012). To ensure data consistency between systems, we adopted lightning strikes rather than flashes in this study.

3.2. WRF setup and sensitivity analysis

We adopted the Advanced Research WRF version 4.0 (Skamarock *et al* 2019) for simulation. The National

Table 1. WRF parameterization schemes used for the pan-Arctic region in existing literature.

Components	Schemes	References
Microphysics	Morrison 2-moment	(Bieniek <i>et al</i> 2016)
	Thompson 2-moment	(Kim <i>et al</i> 2014; Mölders 2010, Mölders 2008)
	WRF single-moment 6-class Goddard Cumulus Ensemble Model	(Hines and Bromwich 2008) (Cassano <i>et al</i> 2011; Glisan <i>et al</i> 2013)
Longwave radiation	Rapid Radiative Transfer Model (RRTM) Longwave	(Bieniek <i>et al</i> 2016; Cai <i>et al</i> 2018; Glisan <i>et al</i> 2013; Hines <i>et al</i> 2011; Kim <i>et al</i> 2014; Mölders 2010, Mölders 2008)
	Community Atmospheric Model (CAM) Longwave RRTM Shortwave	(Cassano <i>et al</i> 2011; Glisan <i>et al</i> 2013) (Bieniek <i>et al</i> 2016; Glisan <i>et al</i> 2013; Kim <i>et al</i> 2014)
Shortwave radiation	Dubhia Shortwave	(Cai <i>et al</i> 2018; Mölders 2010, Mölders 2008)
	Goddard Shortwave CAM Shortwave Grell-Devenyi ensemble	(Hines <i>et al</i> 2011) (Cassano <i>et al</i> 2011; Glisan <i>et al</i> 2013) (Bieniek <i>et al</i> 2016; Cassano <i>et al</i> 2011; Glisan <i>et al</i> 2013)
Cumulus	Kain-Fritsch Mellor-Yamada-Janjic (MYJ)/Monin-Obukhov Eta (Eta)	(Cai <i>et al</i> 2018) (Bieniek <i>et al</i> 2016; Cassano <i>et al</i> 2011; Glisan <i>et al</i> 2013; Hines <i>et al</i> 2011)
	PBL/ Surface layer Yonsei University (YSU)/ Monin-Obukhov MM5 (MM5) Noah	(Cai <i>et al</i> 2018; Kim <i>et al</i> 2014; Mölders 2010, Mölders 2008) (Bieniek <i>et al</i> 2016; Cai <i>et al</i> 2018; Cassano <i>et al</i> 2011; Glisan <i>et al</i> 2013; Hines <i>et al</i> 2011)
Land surface model	Rapid Update Cycle	(Mölders 2010, Mölders 2008)

Table 2. Six candidates of parameterization combinations for sensitivity analysis.

Combination notation	Microphysics	PBL + surface layer
Morrison_MYJ	Morrison 2-moment	MYJ + Eta
Thompson_MYJ	Thompson 2-moment	MYJ + Eta
WRF6_MYJ	WRF6	MYJ + Eta
Morrison_YSU	Morrison 2-moment	YSU + MM5
Thompson_YSU	Thompson 2-moment	YSU + MM5
WRF6_YSU	WRF6	YSU + MM5

Centers for Environmental Prediction Final Operational Model Global Tropospheric Analysis data (NCEP FNL) at $1^\circ \times 1^\circ$ resolution and 6-h interval were used for model initialization (NCEP 2000). We defined two domains with 25 km (Domain 1) and 5 km (Domain 2) grid spacings for two-way nested simulation (figure 1(b)). The vertical dimension was configured with 33 unevenly spaced full sigma levels with the model top defined at 50 hPa.

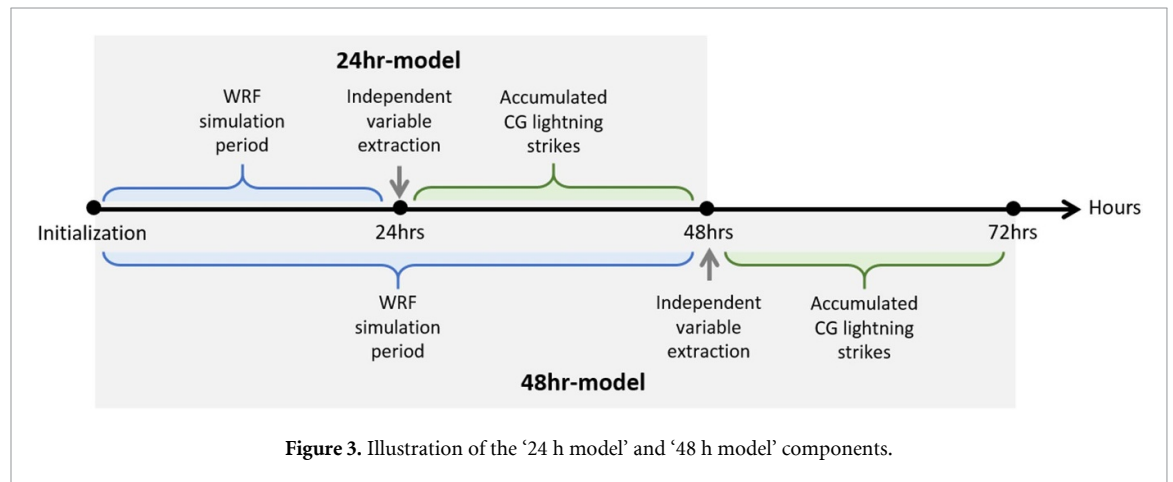
WRF provides multiple parameterization schemes for major physics components (table 1), which can affect simulation results for a specific region given various assumptions and mechanisms. Since existing WRF applications in the HNL primarily focus on the boreal forests or the pan-Arctic region, their schemes may not be suitable for the tundra. Therefore, we conducted a sensitivity analysis to determine WRF settings

that most closely match tundra meteorological observations.

We first identified a list of candidate schemes through literature review, the majority of which utilized the Noah, Rapid Radiative Transfer Model (RRTM), and Grell–Devenyi schemes for land surface model, radiation, and cumulus components, respectively (table 1). We adopted their updated versions in WRF version 4.0. Mixed-phased microphysics schemes are typically recommended for simulating icing or convective conditions at a horizontal resolution finer than 10 km (Skamarock *et al* 2019). We thus selected 2-moment schemes of Morrison, Thompson, and WRF 6-class (WRF6) for microphysics, and considered both Mellor–Yamada–Janjic (MYJ) and Yonsei University (YSU) schemes for planetary boundary layer (PBL) representation in our sensitivity analysis (table 2).

Table 3. Summary of case studies for sensitivity analysis.

Year	Number of RAWS stations	Simulation period (UTC time)
2006	8	08/16 00:00–08/17 00:00
2007	9	05/01 00:00–05/02 00:00
2010	12	07/01 00:00–07/02 00:00
2015	29	06/18 00:00–06/19 00:00

**Figure 3.** Illustration of the '24 h model' and '48 h model' components.

Remote Automated Weather Stations (RAWS; <https://raws.nifc.gov>) provide the densest network of near-surface weather observations across Alaska to date. Four variables, including air temperature (T), dew point temperature (T_d), relative humidity (RH), and solar radiation, were utilized as 'ground truth' for sensitivity analysis. To consider different fire regimes (figure 2), we selected four cases for 24 h simulations in years of varying fire season intensity (2006—low, 2007—moderate, 2010 and 2015—intense, figure 2; table 3). We calculated three statistical metrics for each variable, including root-mean-square error (RMSE), mean absolute error (MAE) and Pearson's r correlation, and ranked them of all candidates for each year from 1 (lowest) to 6 (highest). For each metric, the yearly rankings were summed up to create a single rank sum (ranging from 4 to 24), with the larger value representing better overall performance.

3.3. Random forest modeling of CG lightning probability

We used the RF classification algorithm (Breiman 2001) to model CG lightning probability with WRF-simulated atmospheric variables as predictors. As an ensemble method, RF generates a large number of decision trees through permutation and integrates their results for a more stable modeling performance. Two separate modeling experiments referred to as '24 hr model' and '48 hr model' were designed to compare the consistency of modeling performance and variable importance with different simulation periods (0–24 h and 0–48 h, respectively; figure 3).

For each experiment, atmospheric variables were extracted from WRF outputs (Domain 2) simulated

at 24 h or 48 h after initialization, respectively. Four groups of variables were summarized from literature (Reap 1991, Burrows *et al* 2005, Sousa *et al* 2013, Blouin *et al* 2016), including stability indices, cloud properties, weather conditions at multiple pressure levels (500 hPa, 700 hPa, 850 hPa, and 1000 hPa), and two lightning parameterizations from WRF (table 4). Then we used these predictors to model the presence and absence of lightning strikes during the following 24 h after the timing of variable extraction (figure 3). Lightning points from the ALDN dataset were labeled as presence, while random sample points within tundra with no lightning occurred were labeled as absence.

To ensure the representativeness of our models in describing tundra lightning, three lightning severity levels were identified based on the total number of daily lightning strikes for model training, following a similar method by Farukh *et al* (2011): >2000 strikes per day as severe, 500–2000 strikes per day as moderate, and 0–500 strikes per day as low. For each level, five cases were selected for WRF simulation using a stratified random sampling strategy (table 5). We then randomly selected 70% of presence and absence points for model training and reserved the rest 30% for validation. Training and testing points from all levels were combined for model development and accuracy assessment, respectively. We set the number of trees to 500 and the number of variables at each split as 8 in the RF algorithm.

We reported the out-of-bag (OOB) error rate to evaluate the overall accuracy of model training. For validation, we calculated statistical criteria based on the reserved dataset (tables 6 and 7), and generated receiver operating characteristics (ROC) curves and

Table 4. List of independent variables retrieved from WRF simulation output for RF modeling.

Categories	Abbreviation	Description	
Atmospheric stability indices	CAPE	Convective Available Potential Energy	
	CIN	Convective Inhibition	
	LCL	Lifted Condensation Level	
	LFC	Level of Free Convection	
	TT	Total Totals	
	KI	K Index	
	PLI	Parcel Lifted Index (to 500 hPa)	
	BI	Boyd Index	
	SHOW	Showalter Index	
	CF _{total}	Total cloud cover fraction	
	CF _{high}	High-level cloud cover fraction	
	CF _{mid}	Mid-level cloud cover fraction	
	CF _{low}	Low-level cloud cover fraction	
	Cloud properties	CTT	Cloud top temperature
CTH		Cloud top height	
CTP		Cloud top pressure	
IWP		Ice water path	
LWP		Liquid water path	
ER _{Ice}		Effective radius of cloud ice	
ER _{Water}		Effective radius of cloud water	
Q _{Cloud}		Cloud water mixing ratio	
Q _{Ice}		Ice mixing ratio	
Q _{Rain}		Rain mixing ratio	
BT		Brightness temperature	
T		Air temperature at surface and multiple pressure levels	
T _d		Dewpoint temperature at surface and multiple pressure levels	
T.T _d		Temperature-dewpoint spread at multiple pressure levels	
Weather variables	RH	Relative humidity at surface and multiple pressure levels	
	GPZ	Geopotential height at multiple pressure levels	
	DZ	Thickness between any two pressure layers	
	W	Vertical velocity at multiple pressure levels	
	Helicity	Helicity	
	UH	Updraft helicity	
	Rain	Total precipitation	
	PW	Precipitable water	
	SLP	Sea level pressure	
	Lightning parameterizations	PR92	Flash distribution of CG lightning with PR92 scheme
		LPI	Lightning probability index

Table 5. Cases studies of WRF simulations for CG lightning modeling.

Initialization of simulation (UTC)	Total CG lightning strokes during 0 ~ 24 h	Total CG lightning strokes during 24 ~ 48 h
2003/06/23 00:00	1305	1560
2005/06/11 00:00	732	1027
2005/06/29 00:00	3449	2151
2005/08/16 00:00	5	15
2007/07/04 00:00	4280	479
2007/07/11 00:00	2321	2247
2008/06/25 00:00	2030	295
2009/06/09 00:00	335	64
2010/07/01 00:00	1015	1991
2013/06/20 00:00	3073	3641
2013/08/16 00:00	60	10
2015/07/14 00:00	847	4320
2015/06/21 00:00	974	905
2015/07/23 00:00	175	80
2016/07/11 00:00	93	109

area under the curve (AUC). Moreover, we examined the contribution of predictors in modeling tundra

lightning potential with variable importance quantified by mean decrease in accuracy (MDA).

Table 6. Contingency matrix of variables used to calculate statistical scores.

CG lightning event		Observed	
		Presence	Absence
Predicted	Presence	a (hit)	b (false alarm)
	Absence	c (miss)	d (correct non-event)

Table 7. Statistical criteria used for assessing modeling performance.

Statistical scores	Abbreviation	Formula
Probability of Detection	POD	$a/(a+c)$
Critical Success Index	CSI	$a/(a+b+c)$
False Alarm Ratio	FAR	$b/(a+c)$
False Alarm Rate	F	$b/(b+d)$

3.4. Forecasting capability assessment

In addition to empirical modeling, we tested the capability of our empirical-dynamical method in forward forecasting of CG lightning probability at a future timing by applying the RF model developed for a previous period. Here we utilized the ‘24 hr model’ to forecast the CG lightning probability with atmospheric conditions simulated 48 h after initialization. Statistical criteria listed in table 7 and ROC curves were also generated to quantify the forecasting capability.

4. Results

4.1. Sensitivity analysis of WRF simulation

The results of sensitivity analysis indicate variability in the performance of different WRF schemes by meteorological variables and across cases (figure 4; Tables S1–S4 (available online at <https://stacks.iop.org/ERL/15/115009/mmedia>)). The combined statistical ranking for each variable can range between 4 (the lowest rank across all four sensitivity cases, see table 3) and 24 (the highest rank). Based on the results, Thompson_MYJ and Morrison_MYJ emerged as the strongest performing settings for tundra meteorology simulations (figure 4). Although the majority of the correlation values for all meteorological variables are around 0.7 ~ 0.8, the overall simulation results with all six candidates for T and T_d outperform those for RH and solar radiation according to RMSE and MAE (tables S1–S4). Specifically, Thompson_MYJ shows the best results compared to other schemes for T and T_d (figure 4(a)–(b); Tables S1–S2). For RH, MYJ for the PBL scheme delivers superior results compared to YSU, particularly when combined with the Morrison and Thompson schemes (figure 3(c)). While for solar radiation, the Morrison scheme outperforms other microphysics schemes, followed by Thompson.

Since lightning activity is largely related to convection, we further compared the Thompson_MYJ and Morrison_MYJ schemes by examining the spatial

distribution of convective available potential energy (CAPE) as a representative. Considering that the atmospheric soundings were very sparse in the tundra, and the spatial distribution of CAPE from the two schemes was fairly close, we chose the Thompson_MYJ scheme for further simulation, since it shows a more detailed distribution of CAPE values for describing convective activities (figure 5). The optimized WRF schemes were summarized in table 8.

4.2. Accuracy assessment of RF models

The overall OOB error rate and the class errors suggest high accuracy in predicting CG lightning strikes in Alaskan tundra. The ‘24 hr model’ has an overall error rate of 4.64% and an accuracy of 95.36%. Specifically, the absence of CG lightning has a class error of 7.26%, while that of the presence is only 2.54% (table 9(a)). The overall error rate of the ‘48-hr model’ is 6.81% and the accuracy reaches 93.19%. The class errors of the absence and presence of lightning events are 11.15% and 3.43%, respectively (table 9(b)).

Our validation results against the reserved dataset show high overall accuracy in predicting CG lightning strikes in both models by assessing the statistical metrics (table 10) and the ROC curves (figure 6). We also found a notably stronger performance during severe and moderate lightning days than the low severity level in both models. The ‘24 hr model’ shows an overall probability of detection (POD) of 0.96 and a critical success index (CSI) of 0.91, while the false alarm ratio (FAR) and false alarm rate (F) are below 0.1. The AUC values are above 0.95 across lightning days of all severity levels. The ‘48 hr model’ shows an overall POD value of 0.97 and a CSI of 0.88, while the FAR and F metrics are around 0.1. However, the POD and CSI values are below 0.5 for the low severity cases, much lower than those from the ‘24 hr model’. The AUC values reported from validation data are higher than 0.95 during severe and moderate lightning days while dropping to 0.87 for the low severity level days (table 10).

In addition to the purely statistical accuracy assessment, we generated CG lightning probability maps across the entire Alaskan tundra to visually compare the predicted spatial patterns to observed lightning strike distribution (see an example for a severe lightning day in figure 7).

4.3. Forecasting performance

The forecasting test using the ‘24 hr model’ for the 48-h simulation demonstrates promising forecasting results with our method, with POD and CSI around 0.7 and two false ratios FAR and F below 0.08 (table 11). When separated by different severity levels of lightning days, the forecasting performance is consistent with previously reported results: the accuracy appears to be substantially higher for severe and moderate lightning conditions than low severity days.

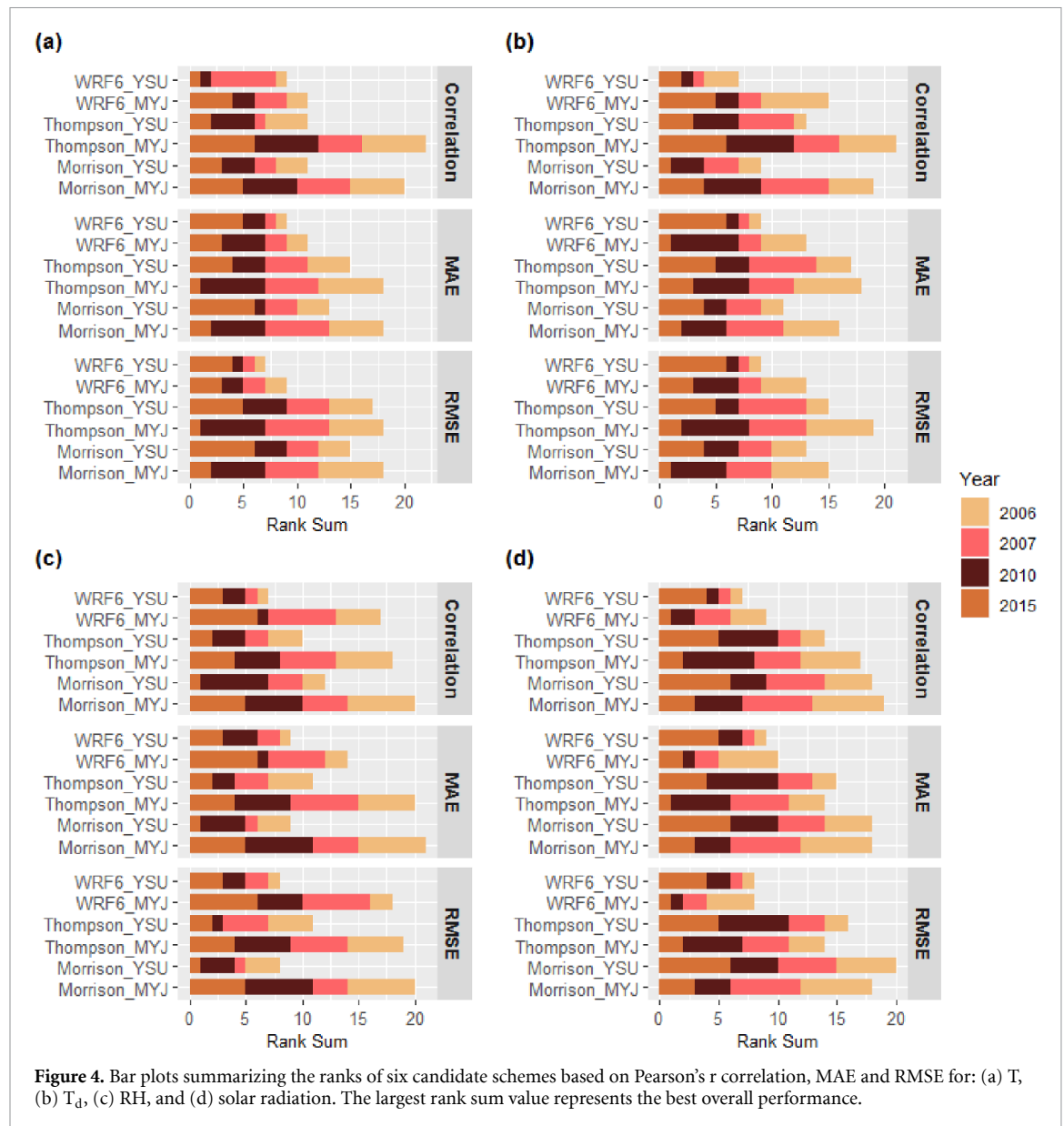


Figure 4. Bar plots summarizing the ranks of six candidate schemes based on Pearson’s r correlation, MAE and RMSE for: (a) T, (b) T_d, (c) RH, and (d) solar radiation. The largest rank sum value represents the best overall performance.

Table 8. Optimized combination of physical parameterizations for WRF.

Physical component	Parameterization scheme	Setting option in WRF
Microphysics	Thompson 2-moment	mp_physics = 8
Cumulus	Grell-Freitas ensemble	cu_physics = 3
PBL	MYJ	bl_pbl_physics = 2
Surface layer	Eta	sf_sfclay_physics = 2
Land surface model	Noah	sf_surface_physics = 2
Longwave radiation	RRTMG	ra_lw_physics = 4
Shortwave radiation	RRTMG	ra_sw_physics = 4

Similar patterns can be found from the ROC curves (figure 8), with the AUC values around 0.9 for the entire data and those from the moderate level cases (table 11).

4.4. Evaluation of variable importance

To understand the predictors’ roles in determining the CG lightning potential in the tundra, we examined the top 20 important variables ranked

according to MDA from both the ‘24 hr model’ and the ‘48 hr model’ for comparison (figure 9). According to both models, the parcel lifted index (PLI) is found to be the most important variable in determining the accumulated lightning strikes among all the predictors. For the ‘24 hr model’, weather variables at multiple pressure levels, including geopotential height (GPZ), T_d, RH, and velocity speed, are also shown as highly important in

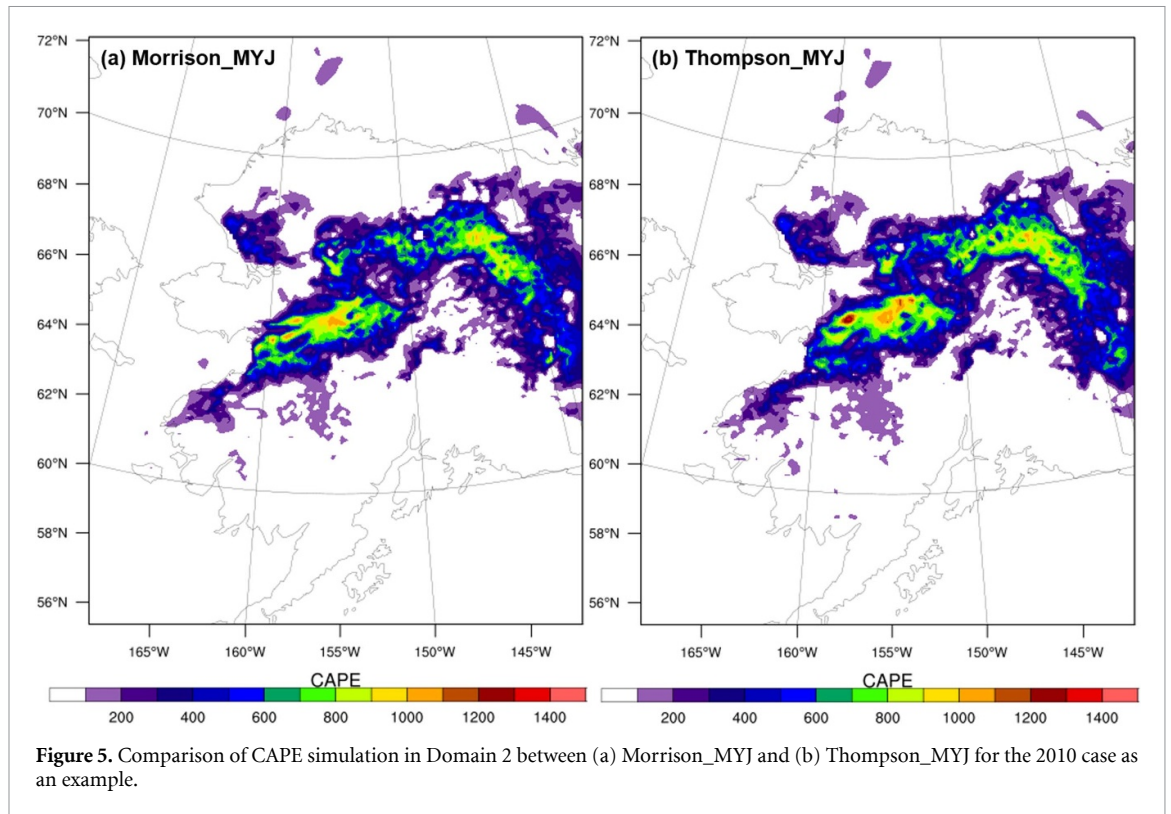


Figure 5. Comparison of CAPE simulation in Domain 2 between (a) Morrison_MYJ and (b) Thompson_MYJ for the 2010 case as an example.

Table 9. Confusion matrices for (a) ‘24 hr model’ and (b) ‘48 hr model’.

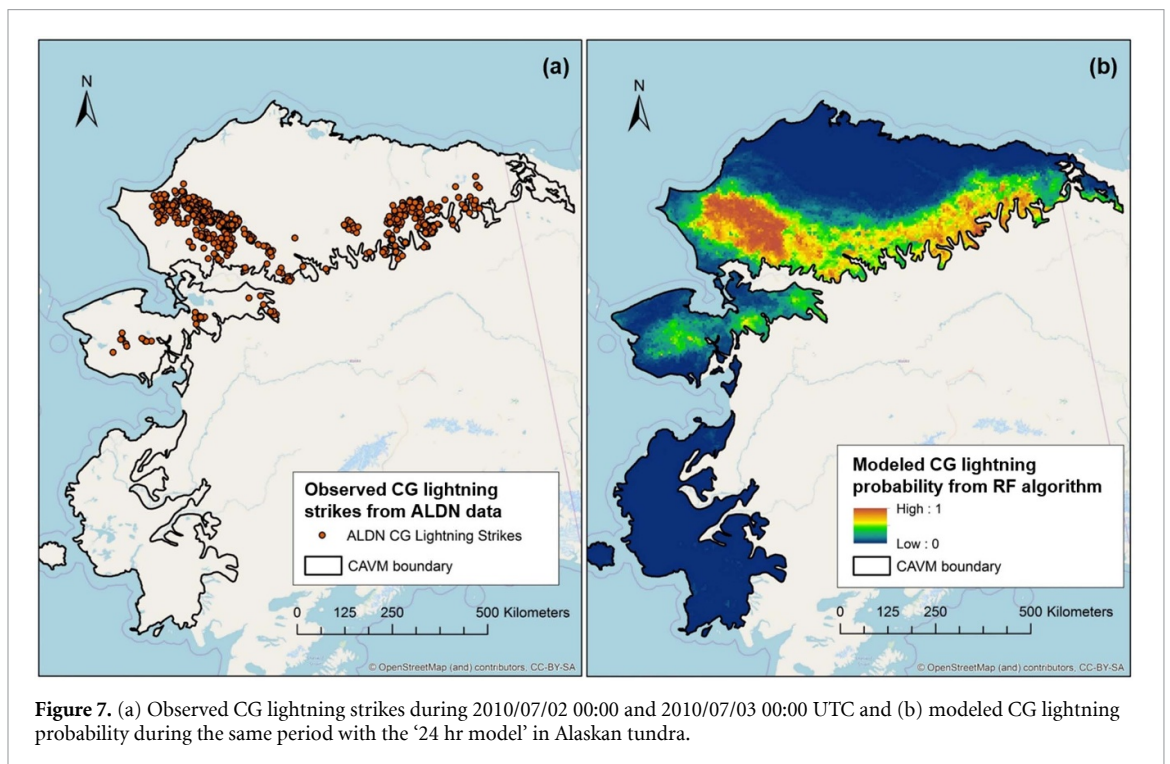
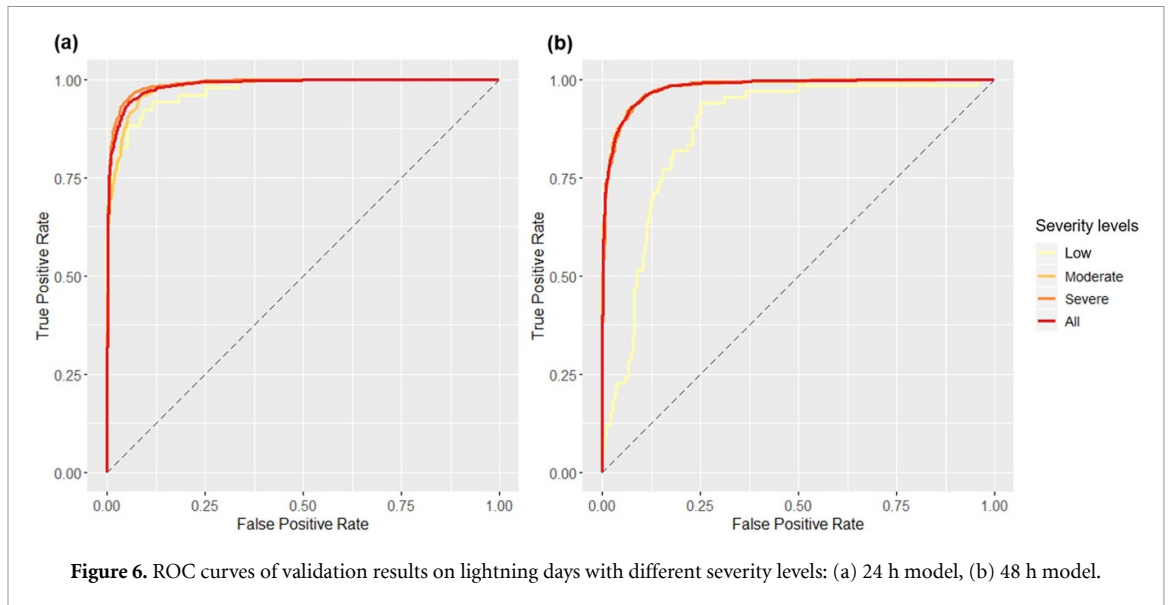
(a) 24 h model				
Confusion matrix		CG lightning predictions		Class error
		Absence	Presence	
CG lightning observations	Absence	7013	549	0.0726
	Presence	241	9239	0.0254
(b) 48 h model				
Confusion matrix		CG lightning predictions		Class error
		Absence	Presence	
CG lightning observations	Absence	4872	612	0.1115
	Presence	243	6837	0.0343

Table 10. Statistical criteria calculated using the validation data for: (a) 24 h model; (b) 48 h model.

Models	Metrics	All	Severe level	Moderate level	Low level
24 h model	POD	0.9628	0.9821	0.9456	0.7885
	CSI	0.9065	0.9365	0.8569	0.7454
	FAR	0.0606	0.0472	0.0987	0.0682
	F	0.0858	0.1167	0.0794	0.0277
	AUC	0.9869	0.9898	0.9818	0.9743
48 h model	POD	0.9668	0.9701	0.9643	0.2273
	CSI	0.8815	0.8808	0.8833	0.1829
	FAR	0.0909	0.0946	0.0868	0.5161
	F	0.1247	0.1291	0.1196	0.0366
	AUC	0.9810	0.9810	0.9809	0.8751

determining CG lightning occurrence in the tundra (figure 9(a)). Also, cloud fraction, sea level pressure, helicity, lifted condensation level, and atmospheric stability indices, such as the Total Totals and the Showalter Index (SHOW), are among the top 20

important predictors. Although the variable ranking order of the ‘48 hr model’ differs from that of the ‘24 hr model’, the majority of the top 20 important variables remain the same. Only layer thickness between 700 hPa and 850 hPa levels



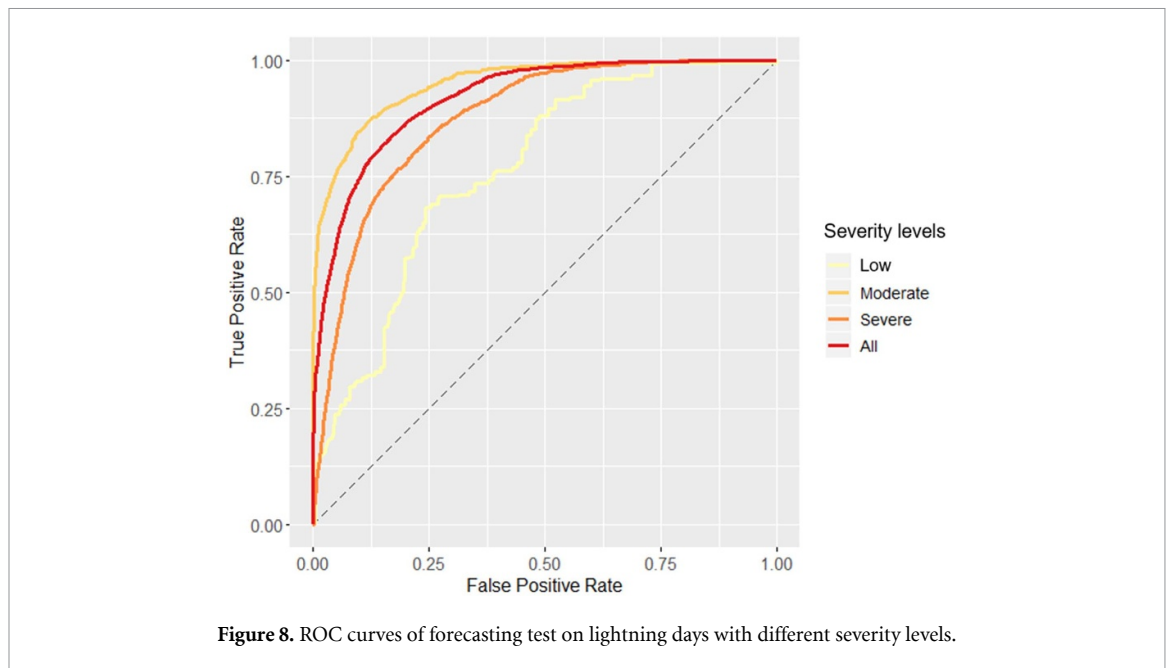
($DZ_{700-850}$) and brightness temperature appear to play an important role in determining the lightning potential for the '48 hr model' but not in the '24 hr model'.

5. Discussions

In general, this study successfully demonstrates the strong capability of the empirical-dynamical framework in representing meteorological conditions that support CG lightning well in Alaskan tundra. By integrating WRF and RF algorithm, our method shows excellent performance in both modeling CG lightning strikes with 24 h and 48 h WRF

simulations, and forward forecasting of lightning probability. This supports the effectiveness of the framework in accurate prediction of future CG lightning potential in data-scarce regions like the HNL.

Our results identify the PLI to 500 hPa as the most important factor in modeling lightning in Alaskan tundra. Similarly, Farukh *et al* (2011) endorsed the lifted index for characterizing lightning in Alaska because of its sensitivity to evaluate upper air instability. This highlights the key role of the lift potential in providing sufficient convection to support lightning formation in the tundra, consistent with the results of Burrows *et al* (2005) in the far west and north region of North



America dominated by tundra. While for boreal forests, SHOW and CAPE were typically recognized as the top-ranking indicators of lightning potential (Burrows *et al* 2005, Blouin *et al* 2016). Compared to static indices like SHOW, PLI can improve forecasting capability, especially during the afternoon (Galway 1956). Though commonly considered a superior measure of instability, CAPE was not found to be very important here. Unlike CAPE that represents integrated parcel buoyancy of the troposphere, PLI is more of a measure of actual ‘instability’ since it represents the potential buoyancy of a parcel at a certain level (Blanchard 1998). The various index performance in these studies may reflect different land-atmosphere energy exchange and convection between tundra and boreal forests, which also affect the boundary conditions in these ecosystems (Thompson *et al* 2004, Beringer *et al* 2005).

Additionally, GPZ at 500 hPa ranks top in determining CG lightning distribution, indicating potential connections between this pressure level and lightning activity in Alaskan tundra. While Burrows *et al* (2005) suggested that the occurrence of lightning was influenced by the interaction between strong convection and precipitable water (PW) in the cloud, here we found much lower rankings of PW than instability indices like PLI and SHOW in both models. This suggests that convection plays a more critical role than PW in determining the lightning potential in the tundra, which is consistent with the findings of Reap (1991). We also found that the vertical profiles of variables like GPZ, RH, T_d , and layer thickness are highly important in modeling lightning activity in the tundra (figure 9). However, neither of the two internal WRF lightning parameterizations (PR92 and LPI) appears to represent lightning potential in

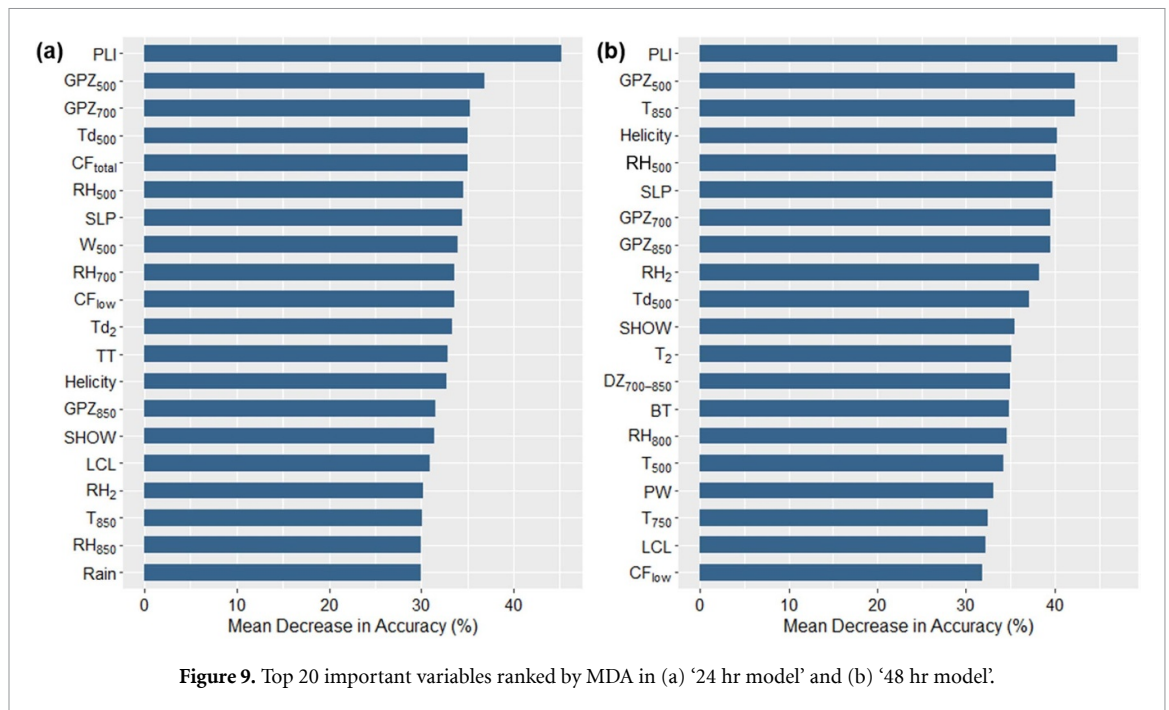
Table 11. Statistical criteria calculated for the forecasting test.

Metrics	All	Severe level	Moderate level	Low level
POD	0.7063	0.6372	0.7707	0.1515
CSI	0.6660	0.5898	0.7397	0.1397
FAR	0.0788	0.1119	0.0516	0.2
F	0.0780	0.1024	0.0547	0.0132
AUC	0.9203	0.8766	0.9519	0.769

the tundra at the regional scale well. This is not surprising as these parameterizations were not specifically developed for the HNL.

Our selection of Thompson 2-moment and MYJ schemes for WRF simulation in the tundra is consistent with the existing findings of WRF applications in lightning modeling. With a more detailed distribution of CAPE values for describing convective activities (figure 4), the Thompson scheme is also recommended by other studies given its detailed representation of ice-phase processes and improved simulation performance for convection related events like precipitation (Zepka *et al* 2014, Giannaros *et al* 2015). For lightning modeling purposes, the MYJ scheme is suitable for describing PBL conditions considering its optimal description of atmospheric conditions for triggering convection activities (Sousa *et al* 2013, Giannaros *et al* 2015).

Despite WRF’s strong capabilities in regional modeling and dynamic downscaling of atmospheric conditions, its performance is affected by the parameterization schemes’ assumptions and mechanisms for describing physical processes. Polar WRF is now under development to improve the representation of near-surface and atmospheric conditions for the Arctic regions, which can support lightning modeling for Alaska in the future (Hines *et al* 2011, Wilson *et al* 2011, Cai *et al* 2018).



Although our modeling results show very impressive prediction capabilities, they are subject to uncertainties inherent in CG lightning observations detected from either the ground-based networks. Although satellite-based sensors such as Lightning Imaging Sensor or Geostationary Lightning Mapper monitor lightning at a large spatial scale, their datasets are not available for the HNL due to the limited spatial coverage and resolution (Nag *et al* 2014, Matsangouras *et al* 2016). Separating the CG and cloud-to-cloud lightning flashes from satellite observations can introduce errors as well (Nag *et al* 2014). Although ground-based systems are constrained by position accuracy and detection efficiency, we found reporting probability a more effective way to describe CG lightning activity.

In addition to atmospheric factors that function as the key predictors for lightning, synoptic-scale dynamic forcings control meteorological mechanisms driving lightning and fire weather (Reap 1994, Flannigan and Wotton 2001, Santos *et al* 2013). For example, Kochtubajda *et al* (2019) found more frequent ridging and ridge displacements during the 2014 wildfire season in the Northwest Territories of Canada. Synoptic weather conditions should be explored and incorporated in future modeling efforts to improve our understanding of lightning and fire regimes in the tundra.

Since CG lightning is the primary ignition source of wildfire in boreal forests and tundra (French *et al* 2015, Veraverbeke *et al* 2017), our integration of NWP and machine learning is easily transferable to monitor and predict fire potential in other data-scarce regions. This provides opportunities for fire management efforts by enhancing our capability to assess future fire impacts on ecosystems and climate

and improving fire prevention and suppression practices. Also, fire prediction can ultimately improve the safety and health of the human communities as an important tool in public health applications. Wildfires in the HNL frequently occur in remote and sparsely populated areas and thus pose little direct threat to life and property. However, emissions can be transported hundreds to thousands of kilometers away, exerting considerable impacts on local and regional air quality and leading to various health outcomes (Morris *et al* 2006, Reisen *et al* 2015).

6. Conclusions

This study makes the first effort in examining the factors driving lightning activity in Alaska tundra with our statistical-dynamical modeling method. We demonstrated the effectiveness of integrating WRF and machine learning for lightning modeling in Alaskan tundra at 5 km spatial resolution. Our results provide insights into understanding the mechanisms of lightning-ignited fires in the tundra. We found PLI and weather variables at multiple pressure levels the most important predictors for modeling lightning potential in the tundra, indicating the primary role of convection in the formation of thunderstorms and CG lightning. Moreover, applicable to other data-scarce regions, our method can further support lightning and fire prediction as well as fire management efforts in the HNL.

Acknowledgments

This work was supported by the NASA Terrestrial Ecology program grant NNX15AT79A.

Data availability statement

The data that support the findings of this study are available upon reasonable request from the authors.

ORCID iDs

Jiaying He  <https://orcid.org/0000-0002-6394-5218>

Tatiana V Loboda  <https://orcid.org/0000-0002-2537-2447>

References

- Anderson K R 1991 Models to predict lightning occurrence and frequency over Alberta MSc thesis University of Alberta
- Anderson K 1992 Forecasting Lightning Occurrence and Frequency 1–18 Proc. 8th Central Region Fire Weather Committee Scientific and Technical Seminar Winnipeg, Manitoba Edmonton Forestry Canada
- Baker M B, Blyth A M, Christian H J, Latham J, Miller K L and Gadian A M 1999 Relationships between lightning activity and various thundercloud parameters: satellite and modelling studies *Atmos. Res.* **51** 221–36
- Barthe C, Deierling W and Barth M C 2010 Estimation of total lightning from various storm parameters: a cloud-resolving model study *J. Geophys. Res.* **115** 1–17
- Bates B C, Dowdy A J and Chandler R E 2018 Lightning prediction for Australia using multivariate analyses of large-scale atmospheric variables *J. Appl. Meteorol. Climatol.* **57** 525–34
- Beringer J, Chapin F S, Thompson C C and McGuire A D 2005 Surface energy exchanges along a tundra-forest transition and feedbacks to climate *Agric. For. Meteorol.* **131** 143–61
- Bieniek P A, Bhatt U S, Walsh J E, Rupp T S, Zhang J, Krieger J R and Lader R 2016 Dynamical downscaling of ERA-interim temperature and precipitation for Alaska *J. Appl. Meteorol. Climatol.* **55** 635–54
- Blanchard D O 1998 Assessing the vertical distribution of convective available potential energy *Weather Forecast* **13** 870–7
- Bliss L C and Hu F S 2020 www.britannica.com/science/tundra Encyclopædia Britannica, inc.
- Blouin K D, Flannigan M D, Wang X and Kochtubajda B 2016 Ensemble lightning prediction models for the province of Alberta, Canada *Int. J. Wildl. Fire* **25** 421–32
- Bond-Lamberty B, Peckham S D, Ahl D E and Gower S T 2007 Fire as the dominant driver of central Canadian boreal forest carbon balance *Nature* **450** 89–92
- Breiman L 2001 Random forests *Mach. Learn.* **45** 5–32
- Bret-Harte M S, Mack M C, Shaver G R, Huebner D C, Johnston M, Mojica C A, Pizano C and Reiskind J A 2013 The response of Arctic vegetation and soils following an unusually severe tundra fire *Philos. Trans. R. Soc. B* **368** 20120490
- Buiat M, Porcù F and Dietrich S 2017 Observing relationships between lightning and cloud profiles by means of a satellite-borne cloud radar *Atmos. Meas. Tech.* **10** 221–30
- Burrows W R, Price C and Wilson L J 2005 Warm season lightning probability prediction for Canada and the Northern United States *Weather Forecast* **20** 971–88
- Cai L, Alexeev V A, Arp C D, Jones B M, Liljedahl A K and Gädeke A 2018 The Polar WRF downscaled historical and projected twenty-first century climate for the coast and foothills of Arctic Alaska *Front. Earth Sci.* **5** 1–15
- Cassano J J, Higgins M E and Seefeldt M W 2011 Performance of the weather research and forecasting model for month-long pan-Arctic simulations *Mon. Weather Rev.* **139** 3469–88
- Dee D, Fasullo J, Shea D and Walsh J (ed) N.C. for A.R.S. 2016 The climate data guide: atmospheric reanalysis: overview & comparison tables
- Di Giuseppe F, Pappenberger F, Wetterhall F, Krzeminski B, Camia A, Libertá G and Miguel J S 2016 The potential predictability of fire danger provided by numerical weather prediction *J. Appl. Meteorol. Climatol.* **55** 2469–91
- Dissing D and Verbyla D L 2003 Spatial patterns of lightning strikes in interior Alaska and their relations to elevation and vegetation *Can. J. For. Res.* **782** 770–82
- Farukh M A, Hayasaka H and Kimura K 2011 Characterization of lightning occurrence in Alaska using various weather indices for lightning forecasting *J. Disaster Res.* **6** 343–55
- Flannigan M D and Wotton B M 2001 Climate, weather, and area burned *Forest Fires* (Amsterdam: Elsevier) pp 351–73
- French N H F, Jenkins L K, Loboda T V, Flannigan M, Jandt R, Bourgeau-Chavez L L and Whitley M 2015 Fire in arctic tundra of Alaska: past fire activity, future fire potential, and significance for land management and ecology *Int. J. Wildl. Fire* **24** 1045–61
- French N H F, Whitley M A and Jenkins L K 2016 Fire disturbance effects on land surface albedo in Alaskan tundra *J. Geophys. Res. Biogeosci.* **121** 841–54
- Fronterhouse B A 2012 Alaska Lightning Detection Network (ALDN) briefing document Ft. Wainwright, AK Bur. L. Manag. Alaska Fire Serv 1–4
- Fuquay D M 1980 Forecasting lightning activity level and associated weather USDA For. Serv. Res. Pap. INT-244
- Galway J G 1956 The lifted index as a predictor of latent instability *Bull. Am. Meteorol. Soc.* **37** 528–9
- Giannaros T M, Kotroni V and Lagouvardos K 2015 Predicting lightning activity in Greece with the Weather Research and Forecasting (WRF) model *Atmos. Res.* **156** 1–13
- Gijben M, Dyson L L and Loots M T 2017 A statistical scheme to forecast the daily lightning threat over southern Africa using the Unified Model *Atmos. Res.* **194** 78–88
- Glisan J M, Gutowski W J, Cassano J J and Higgins M E 2013 Effects of spectral nudging in WRF on arctic temperature and precipitation simulations *J. Clim.* **26** 3985–99
- Goetz S J, Bunn A G, Fiske G J and Houghton R A 2005 Satellite-observed photosynthetic trends across boreal North America associated with climate and fire disturbance *Proc. Natl Acad. Sci. USA* **102** 13521–5
- Gustine D D, Brinkman T J, Lindgren M A, Schmidt J I, Rupp T S and Adams L G 2014 Climate-driven effects of fire on winter habitat for Caribou in the Alaskan-Yukon Arctic *PLoS One* **9** e100588
- He J, Loboda T V, Jenkins L and Chen D 2019 Mapping fractional cover of major fuel type components across Alaskan tundra *Remote Sens. Environ.* **232** 111324
- Hines K M and Bromwich D H 2008 Development and testing of Polar Weather Research and Forecasting (WRF) model. Part I: greenland ice sheet meteorology *Mon. Weather Rev.* **136** 1971–89
- Hines K M, Bromwich D H, Bai L-S, Barlage M and Slater A G 2011 Development and testing of Polar WRF. Part III: arctic land *J. Clim.* **24** 26–48
- Jandt R, Joly K, Meyers C R and Racine C 2008 Slow recovery of lichen on burned caribou winter range in Alaska Tundra: Potential Influences of Climate Warming and Other Disturbance Factors *Arctic, Antarctic, and Alpine Research* **40** 89–95
- Jones B M, Grosse G, Arp C D, Miller E, Liu L, Hayes D J and Larsen C F 2015 Recent Arctic tundra fire initiates widespread thermokarst development *Sci. Rep.* **5** 15865
- Kim C K, Stuefer M, Schmitt C G, Heymsfield A and Thompson G 2014 Numerical modeling of ice fog in interior Alaska using the weather research and forecasting model *Pure Appl. Geophys.* **171** 1963–82
- Kochtubajda B, Stewart R E, Flannigan M D, Bonsal B R, Cuell C and Mooney C J 2019 An assessment of surface and atmospheric conditions associated with the extreme 2014 wildfire season in Canada's Northwest territories *Atmos.-Ocean* **57** 73–90
- Krause A, Kloster S, Wilkenskeld S and Paeth H 2014 The sensitivity of global wildfires to simulated past, present, and

- future lightning frequency *J. Geophys. Res. Biogeosci.* **119** 312–22
- Lynn B H, Yair Y, Price C, Kelman G and Clark A J 2012 Predicting cloud-to-ground and intracloud lightning in weather forecast models *Weather Forecast* **27** 1470–8
- Mack M C, Bret-Harte M S, Hollingsworth T N, Jandt R R, Schuur E A G., Shaver G R and Verbyla D L 2011 Carbon loss from an unprecedented Arctic tundra wildfire *Nature* **475** 489–92
- Matsangouras I T, Nastos P T and Kapsomenakis J 2016 Cloud-to-ground lightning activity over Greece: spatio-temporal analysis and impacts *Atmos. Res.* **169** 485–96
- McGuiney E, Shulski M and Wendler G 2005 Alaska lightning climatology and application to wildfire science: *Proc. of the 85th American Meteorological Society Annual Meeting*
- Mölders N 2008 Suitability of the Weather Research and Forecasting (WRF) model to predict the June 2005 fire weather for interior Alaska *Weather Forecast* **23** 953–73
- Mölders N 2010 Comparison of Canadian forest fire danger rating system and national fire danger rating system fire indices derived from Weather Research and Forecasting (WRF) model data for the June 2005 Interior Alaska wildfires *Atmos. Res.* **95** 290–306
- Morris G A *et al* 2006 Alaskan and Canadian forest fires exacerbate ozone pollution over Houston, Texas, on 19 and 20 July 2004 *J. Geophys. Res. Atmos.* **111** D24S03
- Nag A, Murphy M J, Schulz W and Cummins K L 2015 Lightning locating systems: characteristics and validation techniques *Earth Space Sci.* **2** 65–93
- National Centers for Environmental Prediction/National Weather Service/NOAA/U.S. Department of Commerce 2000 NCEP FNL Operational Model Global Tropospheric Analyses, continuing from July 1999
- Pearson R G, Phillips S J, Lorant M M, Beck P S A, Damoulas T, Knight S J and Goetz S J 2013 Shifts in Arctic vegetation and associated feedbacks under climate change *Nat. Clim. Chang.* **3** 673–7
- Price C and Rind D 1994a Possible implications of global climate change on global lightning distributions and frequencies *J. Geophys. Res.* **99** 10823–31
- Price C and Rind D 1994b Modeling global lightning distributions in a general circulation model *Mon. Weather Rev.* **122** 1930–9
- Racine C H, Johnson L A and Viereck L A 1987 Patterns of vegetation recovery after Tundra fires in Northwestern Alaska, U.S.A. *Arct. Alp. Res.* **19** 461–9
- Rakov V A and Uman M A 2003 *Lightning: Physics and Effects* (Cambridge: Cambridge University Press)
- Reap R M 1991 Climatological characteristics and objective prediction of thunderstorms over Alaska *Weather Forecast* **309**–19
- Reap R M and Foster D S 1979 Automated 12–36 hour probability forecasts of thunderstorms and severe local storms *J. Appl. Meteorol.* **18** 1304–15
- Reap R M and Macgorman D R 1989 Cloud-to-ground lightning: climatological characteristics and relationships to model fields, radar observations, and severe local storms *Mon. Weather Rev.* **117** 518–35
- Reap R 1994 Analysis and prediction of lightning strike distributions associated with synoptic map types over Florida *Mon. Weather Rev.* **122** 1698–715
- Reisen F, Duran S M, Flannigan M, Elliott C and Rideout K 2015 Wildfire smoke and public health risk *Int. J. Wildl. Fire* **24** 1029–44
- Rivas Soriano L, Sánchez Llorente J M, González Zamora A and de Pablo Dávila F 2019 Influence of land cover on lightning and convective precipitation over the European continent *Prog. Phys. Geogr.* **43** 352–64
- Romps D M, Seeley J T, Vollaro D and Molinari J 2014 Projected increase in lightning strikes in the United States due to global warming *Science* **346** 851–4
- Santos J A, Reis M A, De Pablo F, Rivas-Soriano L and Leite S M 2013 Forcing factors of cloud-to-ground lightning over Iberia: regional-scale assessments *Nat. Hazards Earth Syst. Sci.* **13** 1745–58
- Saunders C 2008 Charge separation mechanisms in clouds *Space Sci. Rev.* **137** 335–53
- Schön C, Dittich J and Müller R 2018 The error is the feature: how to forecast lightning using a model prediction error **2979**–88
- Shafer P E and Fuelberg H E 2006 A statistical procedure to forecast warm season lightning over portions of the Florida peninsula *Weather Forecast* **21** 851–68
- Skamarock W C *et al* 2019 A description of the advanced research WRF model version 4 NCAR technical note *Natl. Cent. Atmos. Res.* **145**
- Sly W K 1965 A convective index in relation to lightning strikes in Northwestern Alberta, CIR 4220 TEC 566 Dept. of Transport, Canada 11 pp
- Sousa J F, Frago M, Mendes S, Corte-Real J and Santos J A 2013 Statistical-dynamical modeling of the cloud-to-ground lightning activity in Portugal *Atmos. Res.* **132–133** 46–64
- Thompson C, Beringer J, Chapin F S and Mcquire A D 2004 Structural complexity and land-surface energy exchange along a gradient from arctic tundra to boreal forest *J. Veg. Sci.* **15** 397–406
- Van Heerwaarden C C and Teuling A J 2014 Disentangling the response of forest and grassland energy exchange to heatwaves under idealized land-atmosphere coupling *Biogeosciences* **11** 6159–71
- Veraverbeke S, Rogers B M, Goulden M L, Jandt R R, Miller C E, Wiggins E B and Randerson J T 2017 Lightning as a major driver of recent large fire years in North American boreal forests *Nat. Clim. Chang.* **7** 529–34
- Walker D A and *et al* (The other members of the CAVM team) 2005 The Circumpolar Arctic vegetation map *J. Veg. Sci.* **16** 267–82
- Wilson A B, Bromwich D H and Hines K M 2011 Evaluation of polar WRF forecasts on the arctic system reanalysis domain: Surface and upper air analysis *J. Geophys. Res. Atmos.* **116** D11112
- Wong J, Barth M C and Noone D 2013 Evaluating a lightning parameterization based on cloud-top height for mesoscale numerical model simulations *Geosci. Model Dev.* **6** 429–43 <https://gmd.copernicus.org/articles/6/429/2013/>
- Wotton B M, Nock C A and Flannigan M D 2010 Forest fire occurrence and climate change in Canada *Int. J. Wildl. Fire* **19** 253–71
- Yair Y 2008 Charge generation and separation processes *Space Sci. Rev.* **137** 119–31
- Yair Y, Lynn B, Price C, Kotroni V, Lagouvardos K, Morin E, Mugnai A and Del Carmen Llasat M 2010 Predicting the potential for lightning activity in Mediterranean storms based on the Weather Research and Forecasting (WRF) model dynamic and microphysical fields *J. Geophys. Res. Atmos.* **115** D04205
- Zepka G S, Pinto O and Saraiva A C V 2014 Lightning forecasting in southeastern Brazil using the WRF model *Atmos. Res.* **135–136** 344–62